Astronomy & Astrophysics manuscript no. pradamoroni
September 15, 2009

Very low mass white dwarfs with a C-O core

P. G. Prada Moroni[1,2] and O. Straniero[3]

[1] Physics Department "E. Fermi", University of Pisa, largo B. Pontecorvo 3, I-56127, Pisa, Italy

[2] INFN, largo B. Pontecorvo 3, I-56127, Pisa, Italy
e-mail: prada@df.unipi.it
[3] INAF – Osservatorio Astronomico di Collurania, via Maggini, I-64100, Teramo, Italy
e-mail: straniero@oa-teramo.inaf.it

Received July 8, 2009; accepted September 9, 2009

ABSTRACT

Context. The lower limit for the mass of white dwarfs (WDs) with C-O core is commonly assumed to be roughly 0.5 $M_\odot$. As a consequence, WDs of lower masses are usually identified as He-core remnants.
Aims. However, when the initial mass of the progenitor star is in between 1.8 and 3 $M_\odot$, which corresponds to the so called red giant (RGB) phase transition, the mass of the H-exhausted core at the tip of the RGB is $0.3<M_H/M_\odot<0.5$. Prompted by this well known result of stellar evolution theory, we investigate the possibility to form C-O WDs with mass $M < 0.5\ M_\odot$.
Methods. The pre-WD evolution of stars with initial mass of about 2.3 $M_\odot$, undergoing anomalous mass-loss episodes during the RGB phase and leading to the formation of WDs with He-rich or CO-rich cores have been computed. The cooling sequences of the resulting WDs are also described.
Results. We show that the minimum mass for a C-O WD is about 0.33 $M_\odot$, so that both He and C-O core WDs can exist in the mass range 0.33-0.5 $M_\odot$. The models computed for the present paper provide the theoretical tools to indentify the observational counterpart of very low mass remnants with a C-O core among those commonly ascribed to the He-core WD population in the progressively growing sample of observed WDs of low mass. Moreover, we show that the central He-burning phase of the stripped progeny of the 2.3 $M_\odot$ star lasts longer and longer as the total mass decreases. In particular, the M= 0.33 $M_\odot$ model takes about 800 Myr to exhausts its central helium, which is more than three time longer than the value of the standard 2.3 $M_\odot$ star: it is, by far, the longest core-He burning lifetime. Finally, we find the occurrence of gravonuclear instabilities during the He-burning shell phase.

Key words. Stars: evolution – Stars: white dwarfs – Stars: horizontal-branch – Stars: interiors – Stars: oscillations

1. Introduction

The value for the minimum mass of white dwarfs (WDs) with a carbon-oxygen (C-O) core is commonly agreed to be around 0.5 $M_\odot$ (Weideman 2000, Meng et al. 2008). The main reason for such a belief is a firm result of the theory of stellar evolution and can be easily understood looking at figure 1, which shows the mass of the hydrogen exhausted core M_H at the first thermal pulse on the asymptotic giant (AGB, solid line) and at the tip of the red giant branch (RGB tip, dashed line) as a function of their initial mass. As it is well known, for initial masses lower than 3 $M_\odot$, the value of M_H at the first thermal pulse is nearly constant around 0.55 $M_\odot$, the exact value depending on the chemical composition. This value represents the minimum mass for C-O WDs produced by the evolution of single, low- or intermediate-mass, stars undergoing normal[1] mass loss during the pre-AGB evolution. Nonetheless, anomalous mass loss episodes occurring on the RGB or during the core He-burning phase, as caused by either Roche-lobe overflow in close-binary evolution or tidal stripping in close encounters between stars in high density environments, could interrupt or change the stellar evolution, leading to the production of a smaller remnant. Actually, slightly smaller C-O WDs results from the evolution of a low-mass star (M<1.5-1.7 $M_\odot$, the excact value depends on the composition), which loses its envelope before the onsent of the AGB, the so-called AGB-manqué (Sweigart, Mengel & Demarque 1974, Caloi 1989, Greggio & Renzini 1990, Castellani & Tornambé 1991, Dorman, Rood & O'Connell 1993). Examples of these objects are the extreme horizontal branch stars (EHB) in globular clusters (GCs) and the field subdwarf B stars, which are core He-burning stars with extremely thin hydrogen envelopes that eventually become C-O core WDs of low mass (Castellani & Castellani 1993, Castellani, Luridiana & Romaniello 1994, D'Cruz et al 1996, Brown et al. 2001, Han et al. 2002, Han et al. 2003, Castellani, Castellani & Prada Moroni 2006, Han 2008). But even in such a case, the theory of stellar evolution predicts the existence of a lower limit, since the mass of the H-exhausted core at the He ignition is slightly lower than 0.5 $M_\odot$ [2] for these low-mass stars (Castellani, Chieffi & Straniero 1992, Dominguez et al. 1999, Girardi 1999, Castellani et al. 2000). In practice, if the mass of the electron-degenerate He-rich core were lower, the cooling processes, i.e. the electronic thermal conduction and the plasma neutrino emission, would prevail on the heating caused by the release of gravitational energy, the He burning would be skipped and a He-core WD would be produced.

The scenario described above explains why WDs whose mass is lower than 0.5 $M_\odot$ are commonly believed to have a He-rich core, but this is not the whole story. In fact, stars with

[1] e.g. a Reimers like mass loss rate during the RGB phase.

[2] The exact value depending on the chemical composition: from 0.46 to 0.50 $M_\odot$ for Z=0.04 to Z=0.0001.

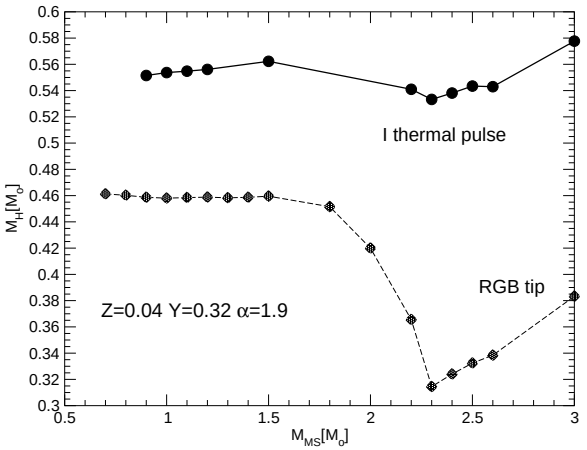

Fig. 1. Mass of the hydrogen exhausted core M_H at the first thermal pulse on the AGB (circles and solid line) and at the tip of the RGB (diamond and dashed line) as a function of the initial mass for stars with Z=0.04 Y=0.32.

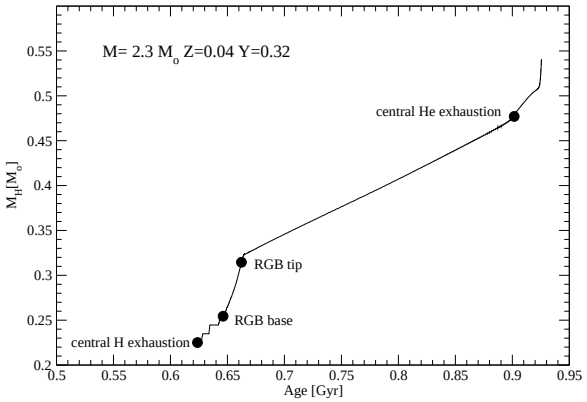

Fig. 2. Mass of the hydrogen exhausted core as a function of the age for a star of M=2.3 $M_\odot$, Z=0.04 Y=0.32.

initial mass in the range 1.8 to 3 $M_\odot$, which undergo intense and rapid mass-loss episode, could produce both CO- or He- rich WDs with mass lower than 0.5 $M_\odot$. In these stars, the degree of electron degeneracy and, in turn, the cooling processes, in the core developed during the RGB are weaker and the He ignition occurs when its mass is lower (see e.g. figure 1). As early as 1985 Iben & Tutukov, in a very instructive paper, showed that a star with an initial mass of 3 $M_\odot$ evolving in a close-binary system can produce a remnant of 0.4 $M_\odot$ with a sizeable C-O core. More recently, Han, Tout & Eggleton 2000, obtain a similar result by computing the evolution of close binary systems by selecting different initial parameters. They showed, in particular, that a star with an initial mass M_1= 2.51 $M_\odot$, belonging to a binary with mass ratio $q=M_1/M_2=2$ and initial period P=2.559 d, eventually succeeds to ignite the helium-burning, even if they did not followed the evolution up to the formation of the C-O WD, since their code met numerical problems when the primary star was as low as 0.33 $M_\odot$ with a C-O core of 0.11 $M_\odot$.

In this framework and by means of detailed computations performed with a full Henyey code able to follow consistently the evolution of stars from the pre-main sequence to the final cooling phase of WDs, we have investigated possible evolutionary scenarios leading to the production of very low mass C-O WDs (VLMWDs), that is with mass lower than < 0.5 $M_\odot$. The peculiar features of the corresponding cooling evolution will be also discussed.

2. The red giant phase transition

The stellar models showed in the present work have been computed with an updated version of FRANEC (Prada Moroni & Straniero 2002, Degl'Innocenti et al. 2008), a full Henyey evolutionary code. We adopted a metallicity Z=0.04 and an initial helium abundance Y=0.32 suitable for the very metal-rich stars belonging to some open galactic cluster, such as NGC6791. A simple way to understand the findings by Iben & Tutukov 1985 and Han, Tout & Eggleton 2000 is to analyze figure 1, which shows the dependence of M_H at the first thermal pulse (solid line) and at the RGB tip (dashed line) on the initial mass for isolated-single stars. At the beginning of the thermally pulsing AGB phase, M_H is almost constant, around 0.55 $M_\odot$, for initial masses lower than 3 $M_\odot$, but at the tip of RGB it presents a deep minimum around 2.3 $M_\odot$, for this particular chemical composition (Sweigart, Renzini and Greggio 1990; Castellani, Chieffi, Straniero 1992, Bono et al. 1997b). Such a behavior is the consequence of the physical conditions occurring in the helium-core at the ignition of the 3α nuclear reaction.

For initial mass lower than 1.5-1.7 $M_\odot$, a regime of strong electron-degeneracy develops in the helium core at the beginning of the red giant phase, and the ignition of the 3α occurs in a violent nuclear runaway, the so-called helium-flash (Hoyle & Schwarzschild 1955) when M_H approaches about 0.46 $M_\odot$, for metal-rich stars, and 0.50 $M_\odot$, for metal-poor stars. The first ignition point is off center and it is followed by a series of weaker and more central flashes, untill a quiescent He burning takes place in the centre. From this point on, the larger the initial mass, the weaker the electron-degeneracy of the core in the red giant phase. Consequently, the mass of the H-exhausted core required for the 3α ignition is smaller and smaller. When the initial mass is as high as about 2.3 $M_\odot$, the helium burning ignites almost quiescently, through a single and central weak flash. For higher masses, the core in the red giant phase is not degenerate any more. Nevertehless, for stars with initial mass larger than about 2.3 $M_\odot$, the larger the initial mass, the larger the M_H at the tip of the RGB. In this stars, indeed, the helium in the core is mainly produced during the central hydrogen-burning phase, which occurs in a convective core whose mass extension is a growing function of the initial total mass. Such a variation of the physical conditions at the He ignition, gives rise to a minimum M_H at the RGB tip that marks the transition between low and intermediate mass stars (the so called RGB phase transition, after Renzini & Buzzoni 1983). For the present composition (Z=0.04 Y=0.32), such a minimum occurs for M=2.3 $M_\odot$ and M_H=0.315 $M_\odot$. The RGB phase transition occurs at larger masses as the initial helium abundance decreases or the initial metallicity increases. Moreover, the value of the minimum M_H at the RGB tip depends slightly on chemical composition (see e.g. Sweigart, Greggio & Renzini 1989). Notice that, as previously stated, this minimum disappears at the first thermal pulse (see the upper curve in figure 1). The reason is that the H-burning shell continues to process hydrogen during the core He burning and move furtherly outward. Moreover, it is a well established result of the theory of stellar evolution that the lower the mass of the H-exhausted core at the onset of the 3α, the fainter the star and the longer the central helium-burning phase. Thus, the H-burning

shell will work for a longer time for stars belonging to the RGB phase transition. This is the reason why stars with initial mass lower than 3 $M_\odot$ enter the AGB phase with nearly the same M_H (Dominguez et al. 1999). Since Iben 1967, who provided the first detailed study of the evolutionary characteristics of stars belonging to the RGB phase transition, many studies were focused on this particular range of stellar mass (see e.g. Sweigart, Greggio & Renzini 1989; Sweigart, Greggio & Renzini 1990; Castellani, Chieffi & Straniero 1992), but only a few dicussed the possible compact remnants of these evolutionary sequences.

Figure 2 illustrates the temporal evolution of the mass of the hydrogen-exhausted core M_H for a star with initial mass 2.3 $M_\odot$. The four circles mark the following evolutionary phases: the central-hydrogen exhaustion, the base and the tip of the RGB, respectively, and the central-helium exhaustion. As one can easily see, when the star exhausts its central hydrogen, the mass of the core is already 0.225 $M_\odot$, which is more than the 70% of the value at the RGB tip. In fact, a sizeable convective core was developed during the previous main sequence phase, which was supported by the H burning through the CNO cycle. When the star reaches the base of the RGB, the mass of the core is 0.254 $M_\odot$, which is about the 80% of the mass at the He ignition, namely 0.315 $M_\odot$.

This means that, since a large fraction of the helium-core required for the ignition of the He-burning is already developed at the beginning of the red giant, a star with mass of about 2.3 $M_\odot$, that undergoes a strong mass loss episode during or immediately after the red giant phase can easily experience the core-He burning phase and produce a C-O VLMWD, that is a C-O WD with a mass substantially lower than 0.5 $M_\odot$, provided that the residual total mass after the anomalous mass loss episode is larger than about 0.32 $M_\odot$.

3. Evolution of the stripped progeny of the 2.3 $M_\odot$ star

In order to check such a working hypothesis and provide models of C-O WDs with mass lower than 0.5 $M_\odot$, we computed the evolution at constant mass of a star with M=2.3 $M_\odot$ until the red giant phase. Then at about $logL/L_\odot$=1.34, when M_H=0.257 $M_\odot$, we switched on a mass loss regime at constant rate, namely: 10^{-7} $M_\odot$ yr^{-1}. Then, we stopped this mass loss regime once required stellar masses was obtained and we followed the next evolution until the final cooling phase. This numerical recipe allowed us to compute a series of starting models of stars that underwent an intense mass loss episode on a time scale much shorter than the evolutionary time scale, as it happens during the Roche-lobe overflow in interacting binary stars or during the tidal stripping caused by close encounters between stars in crowded environment. The details of the rapid mass loss phase are not relevant for the following evolution. We have also checked that the overall evolution of the remnant do not sensibly depends on the luminosity at which the mass loss episode occurs, with the only exception of the smallest model, namely that of M= 0.33 $M_\odot$.

Figure 3 shows the evolutionary tracks in the HR-diagram for different values of the final mass, from 0.5 $M_\odot$ to 0.33 $M_\odot$, from the red giant to the final WD phase. All the models showed in this figure, but that in the bottom-left panel (i.e. panel *g*), succeed to ignite He and become WDs with a C-O core. The evolutionary tracks of the first three models, (those whose remnant mass is 0.5, 0.48 and 0.461 $M_\odot$) respectively, are quite similar. Once the mass loss has been switched off, the star continues to climb the red giant branch until the 3α reactions starts in the centre. The He ignition occurs through a mild flash, which is much weaker than those found in lower mass stars (those developing high-degeneracy conditions), but stronger than that of a normal 2.3 $M_\odot$ star (no anomalous mass loss episodes). Note that the flash is stronger for the smallest remnant. After a few million years since the flash, a quiescent central He-burning phase takes place in a convective core, while, as usual, the H-burning continues in a sorrounding shell. The star moves toward higher effective temperatures until the energy contribution of the 3α nuclear reaction to the total luminosity reached its relative maximum, then it turns-back to the red. The central helium exhaustion is followed by the onset of the He-burning in shell. At this point, the residual hydrogen-rich outer layer is thin, of the order of 0.06 and 0.03 $M_\odot$, for the model of 0.5 and 0.461 $M_\odot$, respectively. The former model attempts to climb the asymptotic giant branch until the thickness of the outer envelope is reduced down to approximately 0.01 $M_\odot$, when it starts to quickly move toward the blue. The latter model, which starts the He-shell burning phase with a much thinner hydrogen-rich envelope, leaves the red side of the HR diagram immediately after the end of the core He-burning. All the 3 models finally approach their WD tracks, where they cool down as a C-O WDs.

From the analysis of these models emerges a general feature, which holds also for the models described in the following of the paper: the lower the mass of the remnant, the lower the mass fraction of the C-O core with respect to the total final mass. Consequently, the thickness of the helium-rich zone gets larger and larger as the mass of the WD decreases. The core of the 0.5 $M_\odot$ WD is about the 91% of the total mass[3], while those of the 0.48 and 0.461 $M_\odot$ are the 89% and the 85%, respectively.

The evolution becomes much more complex and difficult to compute for lower masses, as shown by the looping tracks of the models with remnant mass of 0.43, 0.4 and 0.38 $M_\odot$ plotted in figure 3 (panels *d*, *e* and *f*). The evolution of the 0.43 $M_\odot$ star looks like those described above until the central-He exhaustion, when the model begins to move toward higher effective temperatures. At that point, after four pre-pulses marked by the small zig-zag in the HR diagram, the model experiences a series of 20 He-shell thermal pulses: during each flash the star describes a loop in the HR diagram. Such a series of thermally pulsing loops lasts about 10 Myr. Figure 4 shows the evolutionary track of the 0.43 $M_\odot$ in the HR diagram, zoomed around this phase, and the evolution as a function of time of the total luminosity and the relative contributions of the shell-H burning and of the shell He-brning. After the last of these thermal pulses, the model experiences a couple of post-pulses, again producing small zig-zags in the evolutionary track, followed by a quiescent phase during which the shell He burning provides most of the energy, after an initial short period during which the H shell was dominating. In the meantime, the model moves toward higher effective tempearures approaching the cooling track, where it experiences three strong hydrogen-shell flashes. During these episodes, the residual hydrogen-rich envelope is progressively eroded, until the star can cool down as a WD with a C-O core, whose mass is the 79% of the total mass.

The evolution of the model with 0.4 $M_\odot$ follows qualitatively the same path of the 0.43 $M_\odot$ star, with the difference that, after the thermally pulsing phase, with its characteristic loops in the HR diagram, it experiences a late thermal pulse when the model is already approaching the cooling sequence, as shown in figure 3 (panel *e*). Finally, the star approaches again the cooling track

[3] We define the C-O core as the region where the helium mass fraction is lower than than 0.5

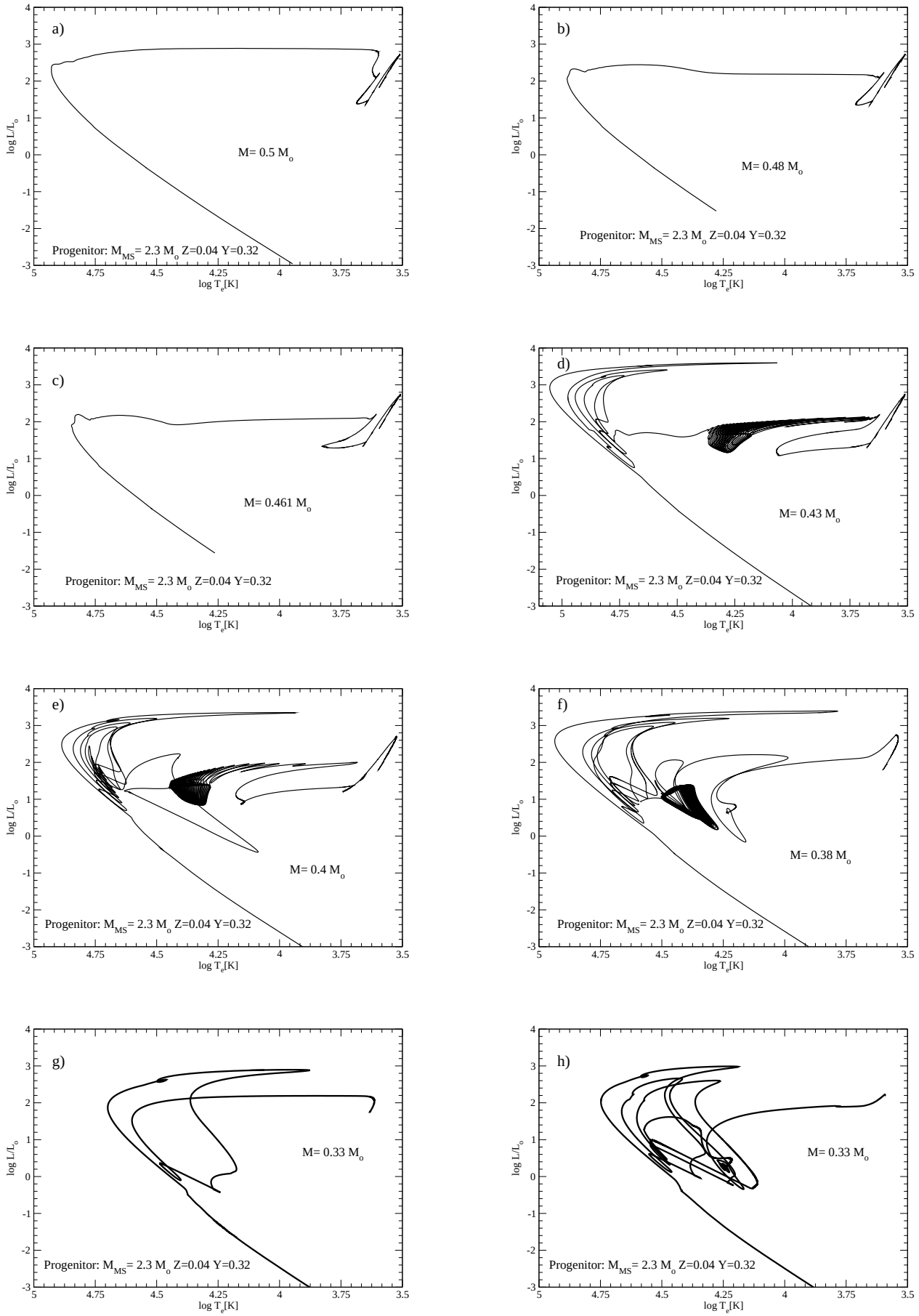

Fig. 3. Evolutionary tracks after the rapid mass loss episode occurred during the RGB of the models described in the text. The labelled masses are final massess or, more specfically, the residual mass after the mass loss episode. In all the cases here illustrated, the progenitor is a star with M_{MS}= 2.3 M_o and Z= 0.04. All the evolutionary models, but the M_f= 0.33 M_o (panel g), produce a C-O

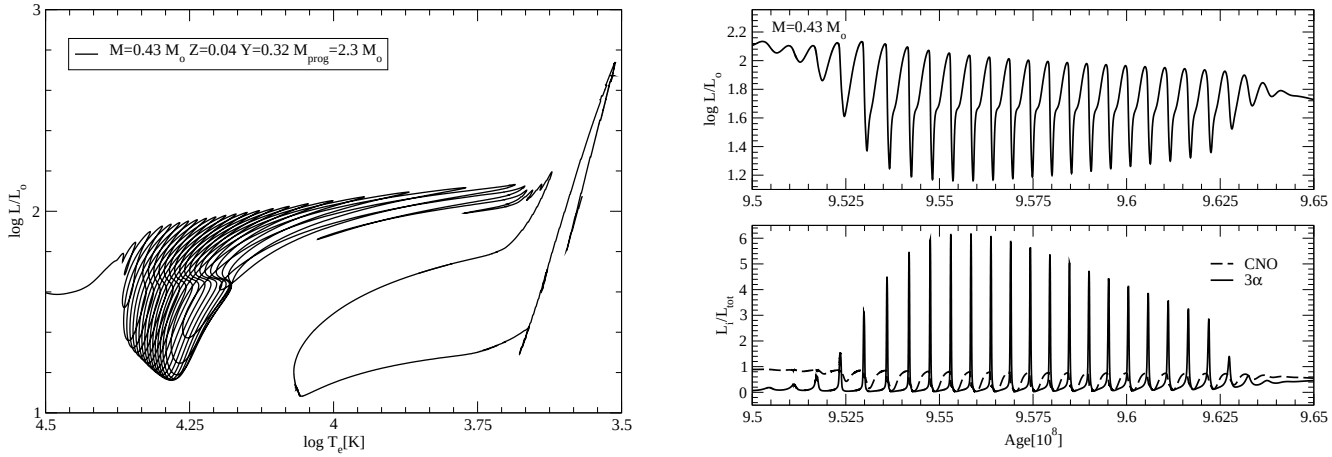

Fig. 4. Model of 0.43 $M_\odot$, whose porgenitor of M= 2.3 $M_\odot$ underwent a strong mass loss episode during the red giant phase. Left panel: evolutionary track in the HR diagram from the RGB phase to the end of the He-thermal pulses. Upper-right panel: evolution of the total luminosity during the thermal pulse phase. Bottom-right panel: Contributions to the total luminosity of the shell-H burning (dashed line) and the shell-He burning (solid line).

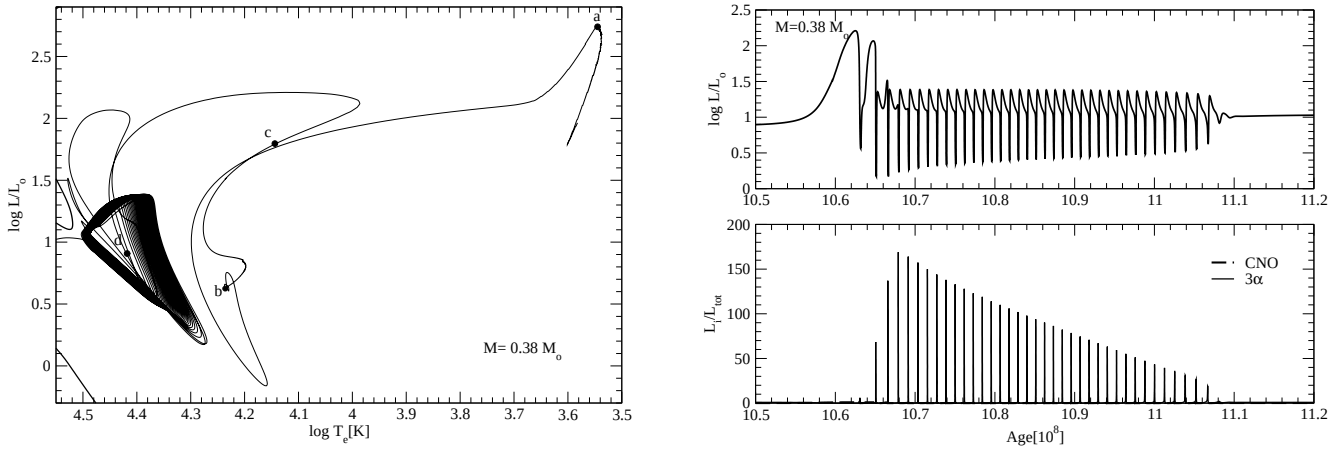

Fig. 5. Same as in figure 4 but for the model of 0.38 $M_\odot$. The He-flash (point a), the beginning (point b) and the end (point c) of the quiescent He-burning in the convective core, the first of the two main He-thermal pulses (point d) are marked.

and experiences a few strong H-shell flashes. The remnant is a WD with a C-O core whose mass is the 70% of the total mass.

The evolution of the model with 0.38 $M_\odot$, shown in figure 5, presents some peculiarities. The ignition of the 3α reaction occurs through a flash, when the star was already leaving the red giant branch (point *a* in figure 5, right-panel). Such an He-flash, although substantially milder than that occurring in low-mass stars, is stronger than those found for the models so far described. The peak of the 3α luminosity is about $8.75 \cdot 10^5$ $L_\odot$, to be compared to that found in the normal 2.3 $M_\odot$ evolution ($3.46 \cdot 10^5$ $L_\odot$) or in the case of the model producing a remnant mass of 0.48 $M_\odot$ ($5.24 \cdot 10^5$ $L_\odot$). The quiescent central He-burning evoltion began after about 5 Myr and proceeds in a convective core for 380 Myr (points *b* and *c* in figure 5). We are witnessing here an important feature of these peculiar objects, which we will discuss later in more detail: the quiescent central He-burning lasts significantly longer than all other models. Point *d* in the figure marks the onset of the first of two main He-thermal pulses, followed by a series of 38 thermal pulses lasting 46 Myr. Once again, during each of these pulses, the model describes a loop in the HR diagram. Notice that the He-thermal pulses we showed above are not the same as that occur in standard AGB stars. In fact, in that case the thermal instability is the consequence of the accumulation of a critical mass of helium accreted by the quiescent hydrogen-burning shell. While in this case the compression is due to the contraction of the core which follows the exhaustion of central helium. To the best of our knowledge, Iben et al. 1986 were the first to show and describe these oscillations following the evolution of a remnant of 0.378 $M_\odot$ with a progenitor of 3 $M_\odot$. Subsequently, Bono et al. 1997a, 1997b, in a couple of papers devoted to the computation of evolutionary and pulsational models of metal-rich stars, showed that the evolution after the central helium exhaustion of models with reduced envelope is characterized by loops in the HR diagram, that they called gravonuclear loops. Since the quoted authors already fully and clearly described these gravonuclear instabilities, we will focus only on the their main features. As early understood in the pioneering study by Schwarzschild & Harm 1965, the ignition

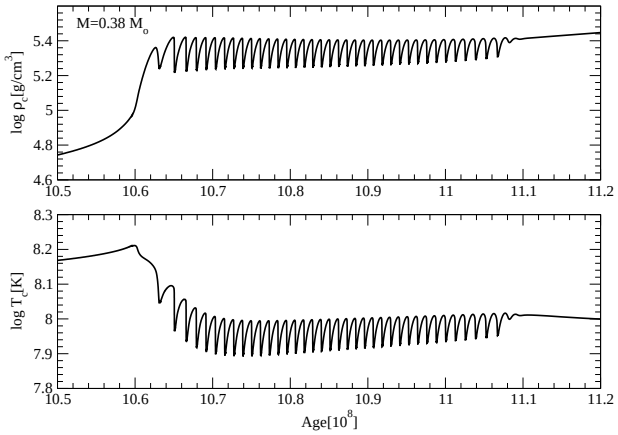

Fig. 6. Model of 0.38 $M_\odot$. Evolution of the central density (in g/cm^3, upper panel) and of the central temperature (in K, lower-panel) during the thermal pulse phase.

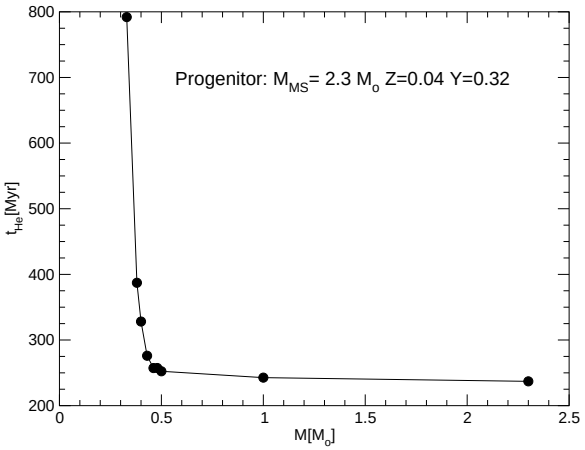

Fig. 7. Helium burning lifetime (in Myr) as a function of the total mass (in $M_\odot$).

of a nuclear reaction (i.e. the 3α), whose efficiency sensitively depends on temperature, in a shell characterized by a steep temperature profile leads to a thermal instability, because the rate at which nuclear energy is released is larger than that at which is dissipated by radiative transfer or converted in work to expand the outer layers. As a consequence the temperature in the burning shell increases, hence the rate of nuclear energy release is further enhanced and a runaway onsets. This is the physical reason at the base of both the standard, and well-known, thermal pulses in AGB stars, and the peculiar, less-known, gravonuclear instabilities. On the other hand, what triggers the instability, i.e. the cause of the compression of the He-shell and the consequent exceeding of the treshold temperature for the nuclear reaction ignition, is different: the accumulation of fresh helium produced by the H-burning shell in normal thermally pulsing AGB stars and the contraction of the core after the central helium exhaustion in the present gravonuclear oscillations. Moreover, at variance with standard thermal pulses, during the loop evolution the H- and He-shell never get near each other and, eventually, the He-burning shell is quenched by the expansion of the envelope. Figure 6 shows the time evolution of the central density (upper panel) and the central temperature (bottom panel) of the 0.38 $M_\odot$ model during the gravonuclear oscillations. As early shown by Iben et al. 1986 and Bono et al. 1997a, 1997b, at variance with standard thermally pulsing phase in normal AGB stars, these pulses affect the entire star, with large oscillations in the central quantities, of the order of 40% in density and 20% in temperature. After the last of these thermal pulses the model gets near to the WD sequence, where it experiences four strong H-flashes and, finally, cools down as WD whose C-O core is only the 50% of the total mass.

Figure 3 (panels *g* and *h*) shows two different evolutionary tracks, corresponding to the same final mass (M= 0.33 $M_\odot$), but leading to the formation of WDs with different composition. In the former case (panel *g* of figure 3), the rapid mass loss episode starts at the same point of the RGB evolution as in all previous cases. This model fails to ignite He in the core and becomes a He WD. In the second model, the rapid mass loss episode on the RGB has been turned on later, when the mass of the H-exhausted core is $\approx$ 1% more massive than in all previous cases. In such a case, the star enters the core-He burning phase (panel *h* of figure 3). When the star is already leaving the RGB, the He ignition occurs through a mild flash. During the flash, an extended convective core (about 80% of the total mass) suddenly appears. Notice the quick decrease of the surface luminosity, due to the temporary stop of the H-burning shell caused by the expansion and the consequent cooling powered by the energetic outcome of the He burning. Then, for a certain time, an oscillation of the He-burning luminosity takes place, correlated to an oscillation of the extension of the convective core and anti-correlated to an oscillation of the gravitational energy release. Meanwhile, the evolutionary track describes small loops in the HR diagram. Later on, a long-lasting quiescent He-burning sets in a convective core, whose maximum mass is about 0.1 $M_\odot$. Once the central He is nearly ehausted, the H-burning shell resumes and becomes the dominant energy source. Approaching the WD sequence, the model experiences three strong H flashes, corresponding to the large loops in the HR diagram. Finally, the star cool down as a WD with a C-O core of about the 53% of the total mass. This is the lowest C-O WD we managed to produce for this chemical composition, since models with mass smaller than 0.33 $M_\odot$ do not ignite the 3α reactions and terminate their evolution as He-core WDs.

Let us stress two peculiar properties of the C-O VLMWDs. Figure 7 shows the duration of the central He-burning t_{He} as a function of the total mass of the remnant obtained by stripping part of the envelope mass along the RGB of a progenitor star with initial mass 2.3 $M_\odot$, whose evolution has been discussed above. As already noted, the smaller the remnant mass the larger the time spent by the models in the central He-burning phase. Such an increase is quite smooth and shallow for remnant mass larger than 0.5 $M_\odot$, but becomes very steep for smaller masses. The smallest models which succeeds to ignite He-burning, that is the M= 0.33 $M_\odot$, takes about 800 Myr to exhausts its central helium, which is more than three time longer than the value of the standard 2.3 $M_\odot$ star. Note that for this peculiar star, the core He-burning lasts more than the central-H burning of the progenitor ($\tau_H \approx 613$ Myr). It is, by far, the longest core-He burning lifetime. As previously recalled, the He-burning lifetime depends on the stellar luminosity, which is smaller for star with smaller H-exhausted core at the He ignition. Thus, looking at the core masses plotted in figure 1, it results that the longest He-burning lifetime for standard models is attained by the star with about 2.3 $M_\odot$, the one corresponding to the minimum of the RGB fase

Table 1. He-burning ignition.

$M[M_\odot]^a$	$M_H[M_\odot]^b$
0.330	0.323
0.380	0.327
0.400	0.325
0.430	0.326
0.461	0.326
0.480	0.326
0.500	0.325
2.300	0.323

[a] stellar mass

[b] mass of the H-exhausted core. As a reference evolutionary point we chose the model in which the central He abundance decreased of 0.001 from the initial value.

transition (Castellani, Chieffi, Straniero 1992; Castellani et al. 2000; Dominguez et al. 1999; Girardi 1999). Table 1 lists the mass of the H-exhausted core M_H, taken at the time when the central He abundance decreased of 0.001 from the initial value, for models of different total mass M. As one can see, at the He ignition, all the models here presented have, more or less, the same core mass of the standard 2.3 $M_\odot$ model. Nonetheless, the substantial erosion of the H-rich envelope causes a depression of the shell-H burning that is more evident for models producing smaller remnants. As a consequence, the rate of growth of the M_H core during the central He-burning, and thus the luminosity evolution and the length of this phase, is quite different in remnants with different envelope thicknesses. The lower the mass of the remnant, the less efficient the H-burning shell and the slower the increase of the M_H core. In the extreme case of the 0.33 $M_\odot$ model, the mass of the H-exhausted core remains almost constant during the entire central He-burning, as the H-shell is pratically turned off. This explains the steep growth of the central He-burning lifetime t_{He} as the mass of the remnants decreases below 0.5 $M_\odot$. Note that, due to the very long He-burning lifetime, the age of the 0.33 $M_\odot$ model at the beginning of the cooling sequence is 1.5 Gyr, to be compared with the 0.9 Gyr of the standar 2.3 $M_\odot$ model, which is expected to produce a C-O WD of about 0.6 $M_\odot$.

Another interesting feature of the C-O VLMWDs concerns their internal composition. Figure 8 shows the chemical abundance profiles of ^{4}He, ^{12}C and ^{16}O of the C-O WD of 0.33 $M_\odot$. As previously stated, the lower the mass of the remnant, the lower the fraction of the total mass confined in to the C-O core or, equivalently, the larger the fraction of mass confined in to the helium-rich external layer. In the case of the 0.33 $M_\odot$ model, the He-rich layer is about the 50% of the total mass, that is very different from the value found for the more massive (normal) C-O WDs, namely 1-2 %.

4. Cooling evolution

The present evolutionary computations confirm that it is possible to have C-O WDs with mass as low as 0.33 $M_\odot$, significantly lower than 0.5 $M_\odot$, the classical and commonly accepted lower limit. This means that in the mass range 0.33 - 0.5 $M_\odot$ both He and C-O core WDs can exist. We will focus on the comparison between the structure and evolution of the two remnants of 0.33 $M_\odot$ with different core compositions.

The thickness of the H-rich outermost layer of the two models of 0.33 $M_\odot$ is practically the same, namely M= 0.0014 M_{WD} for the He WD and M= 0.0015 M_{WD} for the C-O WD. Figure 9

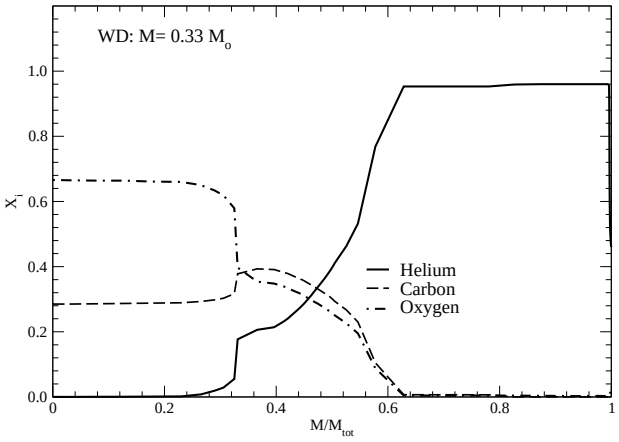

Fig. 8. Internal mass fraction of helium (solid line), carbon (dashed line) and oxygen (dot-dashed line) as a function of the mass coordinate for the C-O WD with M= 0.33 $M_\odot$.

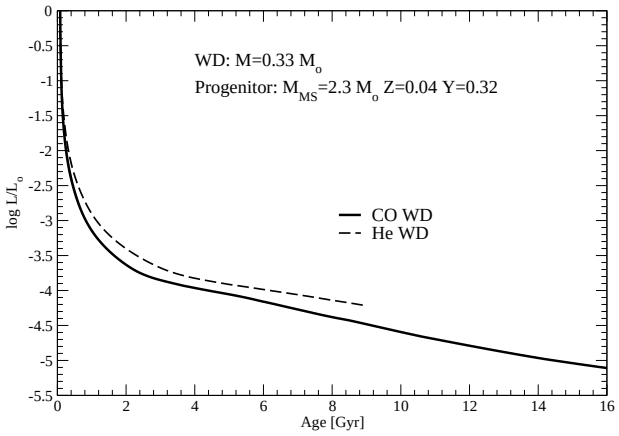

Fig. 9. Comparison between the cooling curves, $\log L/L_\odot$ vs. time, of the two WDs of 0.33 $M_\odot$, that with the He-core (dashed line) and with C-O core (solid line).

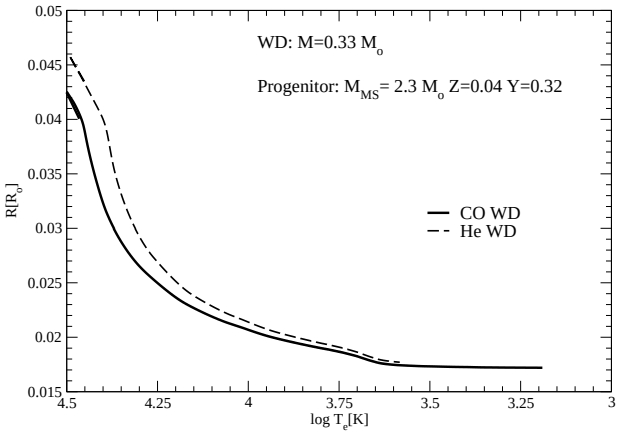

Fig. 10. Radius vs. effective temperature of the two WDs of 0.33 $M_\odot$, that with the He-core (dashed line) and with C-O core (solid line).

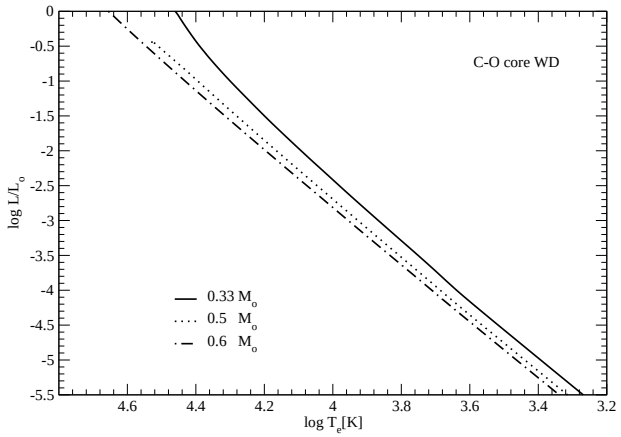

Fig. 11. Comparison between the cooling tracks of C-O core WDs of masses: 0.33 $M_\odot$ (solid line), 0.5 $M_\odot$ (dotted line), 0.6 $M_\odot$ (dot-dashed line).

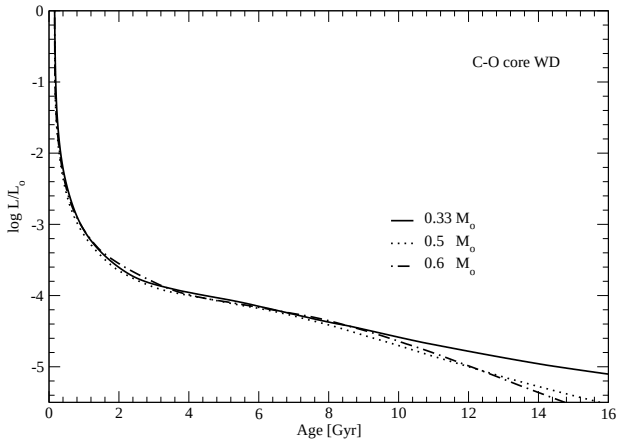

Fig. 12. Comparison between the cooling curves, $logL/L_\odot$ vs. time, of C-O core WDs of masses: 0.33 $M_\odot$ (solid line), 0.5 $M_\odot$ (dotted line), 0.6 $M_\odot$ (dot-dashed line).

shows the comparison between the cooling curves of the He-core WD (dashed line) and the C-O core (solid line). As expected (see the detailed discussion by Panei et al. 2007), the remnant with the He-rich core cools slower than that with a C-O core, as due to the larger specific heat, so that the thermal content of the He WD is larger than that of the C-O one with the same total mass. Such a difference in the cooling times is partially counterbalanced at $logL/L_\odot \approx$ -4, when the C-O core begins to crystallize.

Figure 10 shows the comparison between the radii as a function of the effective temperature for the two WDs of 0.33 $M_\odot$. For a given effective temperature, the He-core WD is more expanded than the other one, the difference beeing not negligible at the beginning of the cooling ($\sim$ 8.5%). In principle, this difference of the radii at a given effective temperature offers the possibility to distinguish the core composition of WDs in the mass range 0.33 - 0.5 $M_\odot$. Since the C-O VLMWDs are the result of non-standard evolutionary channels, it might be of some interest to compare their main characteristics to those of the C-O WDs produced by the evolution of non-interacting-single stars (i.e. WD with mass M$\geq$ 0.5 $M_\odot$). Figures 11 and 12 show the comparison between the tracks in the HR diagram and the cooling curves, respectively, of the lowest C-O core WD we managed to build, namely that of 0.33 $M_\odot$, with the more standard 0.5 and 0.6 $M_\odot$ remnants. As it is expected, the evolutionary tracks of the low mass C-O WD is redder than those of the more massive objects and marks the reddest frontier of the C-O WD loci. The tracks of these peculiar objects overlap the region of the HR diagram occupied by the He WDs. Concerning the comparison among the cooling curves, as shown in figure 12, the luminosity evolutions look like quite similar, although not identical, down to $logL/L_\odot \approx$ -4.4. Then, at fainter magnitudes or for cooling ages larger than $\approx$ 9 Gyr, the evolution of the standard WDs get faster and faster and their luminosity drop more quickly than that of the 0.33 $M_\odot$ model. When the cooling age is 14 Gyr, the 0.6 $M_\odot$ WD reaches $logL/L_\odot \approx$ -5.4, while the 0.33 $M_\odot$ one is still at -4.9. The reason for such a behavior is that the solid core of the VLMWD is less dense than those of the other two objects [4], an occurrence causing a delay of the onset of the Debye-cooling regime. This difference in the luminosity becomes even more large when the longer lifetime of the progenitors of the VLMWDs is taken in to account.

5. Summary and conclusions

By means of fully consistent evolutionary computations, we proved that the minimum mass for a C-O WD is much lower than the commonly agreed 0.5 $M_\odot$. In fact, we described the evolutionary paths leading to the production of C-O WDs with mass as low as 0.33 $M_\odot$, nearly the value of the minimum M_H required for the He ignition in non-degenerate conditions, which depends only slightly on the chemical composition. These VLMWDs with a C-O core might result from the evolution of a star with initial mass around 2.3 $M_\odot$, which undergoes a considerable mass loss along the red giant phase.

As a consequence, in the mass range 0.33-0.5 $M_\odot$ both He and C-O core WDs can exist. As expected and already shown by the detailed analysis of Panei et al. 2007, the cooling times of these two classes of WDs are quite different, being the He-core remnants significantly slower than the C-O ones. Furthermore, we showed also that the He WDs are more expanded that their C-O counterparts at a given effective temperature. In principle, such an occurrence would allow to discriminate between WDs with an He-core and those with a C-O-core in the mass range where both remnants exist, namely 0.33-0.5 $M_\odot$.

Large samples of observed VLMWDs (M<0.5 $M_\odot$), belonging to the field (Liebert et al. 2005, Maxted et al. 2005, Eisenstein et al. 2006) or to stellar clusters (Bedin et al. 2005, Monelli et al. 2005, Kalirai et al. 2007, Bedin et al. 2008, Calamida et al. 2008) are now available. In the next future, basing on the models here discussed, it would be possible to identify the observational counterpart of very low mass remnants with a C-O core among those commonly ascribed to the He-core WD population.

The computation of the evolution of the stripped progeny of the 2.3 $M_\odot$ provided also the evidence for the longest lasting central He-burning stellar objects. In fact, we showed that the smaller the remnant mass, the longer the central He-burning phase. Such an increase becomes very steep for masses lower than 0.5 $M_\odot$ and reaches the maximum for the M= 0.33 $M_\odot$ model, which takes about 800 Myr to exhausts its central helium, which is more than three time longer than the time required

[4] the central density of the 0.6 WD is $\approx$ 5 times larger than that of the 0.33 WD

by the longest lasting He-burning standard star, i.e. the 2.3 $M_{\odot}$. Thus, the M= 0.33 $M_{\odot}$ model attains the longest core He-burning lifetime.

Acknowledgements. It's a pleasure to thank Giuseppe Bono and Scilla Degl'Innocenti, who kindly read the paper, for the many useful and pleasant discussions and the referee (Han Zhanwen) for the positive and useful report. PGPM has been supported by PRIN-MIUR 2007 (*Multiple stellar populations in globular clusters: census, characterizations and origin*, PI G. Piotto), and OS by the PRIN-INAF program 2008.

References

Bedin, L. R., King, I. R., Anderson, J., Piotto, G., Salaris, M., Cassisi, S., Serenelli, A. 2008, ApJ, 678, 1279
Bedin, L. R., Salaris, M., Piotto, G., King, I. R., Anderson, J., Cassisi, S., Momany, Y. 2005, ApJ, 624L, 45
Bono, G., Caputo, F., Cassisi, S., Castellani, V., Marconi, M. 1997, ApJ, 479, 279
Bono, G., Caputo, F., Cassisi, S., Castellani, V., Marconi, M. 1997, ApJ, 489, 822
Brown, T. M., Sweigart, A. V., Lanz, T., Landsman, W. B., Hubeny, I. 2001, ApJ, 562, 368
Calamida, A.; Corsi, C. E.; Bono, G.; Stetson, P. B.; Prada Moroni, P.; et al. 2008, ApJ, 673L, 29
Caloi, V. 1989, A&A, 221, 27
Castellani, M., & Castellani, V. 1993, ApJ, 407, 649
Castellani, M., Castellani, V., & Prada Moroni, P. G. 2006, A&A, 457, 569
Castellani, V., Chieffi, S. & Straniero, O. 1992, ApJSS, 78, 517
Castellani, V., Degl'Innocenti, S., Girardi, L., Marconi, M., Prada Moroni, P. G., Weiss, A. 2000, A&A, 354, 150
Castellani, V., Luridiana, V., Romaniello, M. 1994, ApJ, 428, 633
Castellani, M. & Tornambé, A. 1991, ApJ, 381, 393
Catalan, S., Isern, J., Garcia-Berro, E. & Ribas, I. 2008, MNRAS, 387, 1693
D'Cruz, N. L., Dorman, B., Rood, R. T., O'Connell, R. W. 1996, ApJ, 466, 359
Degl'Innocenti, S., Prada Moroni, P. G., Marconi, M. & Ruoppo, A. 2008, Ap&SS, 316, 25
Dominguez, I., Chieffi, A., Limongi, M. & Straniero, O. 1999, ApJ, 524, 226
Dorman, B., Rood, R. T. & O'Connell, R. W. 1993, ApJ, 419, 596
Eisenstein, D. J., et al. 2006, ApJS, 167, 40
Girardi, L., 1999, MNRAS, 308, 818
Greggio, L. & Renzini, A. 1990, ApJ, 364, 35
Han, Z. 2008, A&A, 484, L31
Han, Z., Podsiadlowski, P., Maxted, P. F. L., Marsh, T. R., Ivanova, N. 2002, MNRAS, 336, 449
Han, Z., Podsiadlowski, P., Maxted, P. F. L., Marsh, T. R. 2003, MNRAS, 341, 669
Han, Z., Tout, C. A. & Eggleton, P. P. 2000, MNRAS, 319, 215
Hoyle, F. & Schwarzschild, M. 1955, ApJS, 2, 1
Iben, I. Jr 1967, ApJ, 147, 650
Iben, I. Jr, Fujimoto, M. Y., Sugimoto, D. & Miyaji, S. 1986, ApJ, 304, 217
Iben, I. Jr & Tutukov, A. V. 1985, ApJSS, 58, 661
Kalirai, J. S., Bergeron, P.; Hansen, B. M. S., Kelson, D. D., Reitzel, D. B., Rich, R. M., Richer, H. B. 2007, ApJ, 671, 748
Liebert, J., Bergeron, P., Holberg, J. B. 2005, ApJS, 156, 47
Maxted, P. F. L., Marsh, T. R., Moran, C. K. J 2005, MNRAS, 319, 305
Meng, X., Cheng., X. & Han, Z. 2008, A&A, 487, 625
Monelli, M., Corsi, C. E., Castellani, V., Ferraro, I., Iannicola, G., Prada Moroni, P. G., et al. 2005, ApJ, 621L, 117
Panei, J. A., Althaus, L. G., Chen, X. & Han, Z. 2007, MNRAS, 382, 779
Prada Moroni, P. G. & Straniero, O. 2002, ApJ, 581, 585
Prada Moroni, P. G. & Straniero, O. 2007, A&A, 466, 1043
Renzini, A. & Buzzoni, A. 1983, memSAIT, 54, 739
Schwarzschild, M. & Harm, R. 1965, ApJ, 142, 855
Sweigart, A. W., Greggio, L., & Renzini, A. 1989, ApJS, 69, 911
Sweigart, A. W., Greggio, L., & Renzini, A. 1990, ApJ, 364, 527
Sweigart, A. W., Mengel, J. G., & Demarque, P. 1974, A&A, 30, 13
Weidemann, V. 2000, A&A, 363, 647